ICARUS **132,** 378–387 (1998)
ARTICLE NO. IS975872

Meteorite Delivery via Yarkovsky Orbital Drift

Paolo Farinella

Dipartimento di Matematica, Università di Pisa, Via Buonarroti 2, 56127 Pisa, Italy
E-mail: paolof@dm.unipi.it

David Vokrouhlický

Institute of Astronomy, Charles University, V Holešovičkách 2, CZ-18000 Prague 8, Czech Republic

and

William K. Hartmann

Planetary Science Institute, 620 North Sixth Avenue, Tucson, Arizona 85705–8331

Received May 23, 1997, revised September 25, 1997

We provide a unified discussion of the Yarkovsky effect in both the original, ''diurnal'' variant and also for the ''seasonal'' variant which has been recently shown by Rubincam (1995) to be important for meteorite-sized, regolith-free asteroid fragments. After computing the rate of the corresponding semimajor axis drift as a function of size and spin rate, and comparing the relevant time scales with those for collisional disruption and spin reorientation, we discuss some issues in meteorite science which are put in a new light by the relevance of the Yarkovsky effect. In particular, this mechanism provides a good explanation for the fact that meteorite cosmic ray exposure ages (in particular for irons) are much longer than the dynamical lifetimes of objects delivered to the Earth-crossing region through resonances. Thanks to the Yarkovsky effect, small asteroid fragments in the belt undergo a slow drift in semimajor axis (with a random-walk component related to their rotational state) and therefore have enough mobility to reach the resonances after comparatively long times spent in nonresonant main-belt orbits. Metal-rich fragments have slower Yarkovsky drift rates than stones, but their much longer collisional lifetimes may explain why iron meteorites appear to sample a larger number of asteroid parent bodies compared to ordinary chondrites.

1. INTRODUCTION

The canonical view of meteorite delivery from the main asteroid belt to Earth (see, e.g., Greenberg and Nolan 1989, Farinella *et al.* 1993a,b) appeals to a combination of collisionally imparted ΔV's to asteroid fragments and their subsequent chaotic orbital evolution due to gravitational perturbations by the planets. Here we shall argue that an important ingredient is probably missing from this general picture: nongravitational orbital drift caused by the so-called Yarkovsky mechanism. As we shall show, this mechanism can cause significant changes in the orbits of rotating asteroid fragments in the size range roughly 0.1 to 100 m, because of the asymmetry between the direction of absorption of sunlight and the direction of reradiated thermal infrared radiation. This size range includes the typical preatmospheric sizes of meteorites, and therefore if this mechanism is as significant as has been calculated, it can lead to some important, but so far underappreciated changes in the canonical view of meteorite delivery from the asteroid belt.

The Yarkovsky effect has been known but obscure for many years. It was pointed out by a Polish engineer, I. O. Yarkovsky, around 1900 and described in a paper that was apparently lost, according to Öpik (1951). Radzievskii (1952), Peterson (1976), Burns *et al.* (1979), and Afonso *et al.* (1995) studied it in more detail, concluding that it may be important for the delivery of meteorites from the asteroid belt. Recent work by Rubincam (1995) and Vokrouhlický and Farinella (in preparation) has shown that in many realistic cases, the original formulation of Yarkovsky (adopted as well in the subsequent investigations listed above) does not apply, and a ''seasonal'' variant of the effect, sometimes also called *thermal drag* mechanism (see below), is the dominant one. It is interesting to recall that the original studies on this latter mechanism (Rubincam 1987, 1988) were aimed at understanding the observed long-term semimajor axis decay of an artificial satellite, *Lageos*, for which very accurate orbital data were available, and that this is still a very active research field to date (see Farinella *et al.* 1996, Farinella and Vokrouhlický 1996, Vokrouhlický and Farinella 1997).

0019-1035/98 $25.00

Complex numerical modeling would be needed to explore fully some of the consequences of the Yarkovsky effect, but we believe it is worthwhile reviewing some of the possibilities in this preliminary survey. In particular, an important conclusion is that this nongravitational mechanism can explain the apparent paradox that most meteorite cosmic-ray exposure ages are much longer than the typical dynamical lifetimes of asteroid fragments once they have been inserted into resonant orbits.

The remainder of this paper is organized as follows. In Section 2 we discuss the thermal parameters controlling the magnitude of the Yarkovsky effect as a function of body size, and in Section 3 we give explicit formulae for the semimajor axis drift rates corresponding to the "diurnal" and "seasonal" variants of the mechanism. These formulae are applied with parameters appropriate for asteroid fragments in Section 4, whereas in Section 5 we estimate the corresponding time scales for collisional disruption and spin axis reorientation. Finally, in Section 6 we discuss the relevance of our results for the meteorite delivery problem.

2. THERMAL PARAMETERS

The physics of the Yarkovsky effect can be summarized as follows. When a solid body (of density ρ, specific heat C, thermal conductivity K) is illuminated by a visible radiation flux varying with a typical frequency ν, its temperature is modified in a surface layer of characteristic thickness

$$l_S = \sqrt{\frac{K}{\rho C \nu}}. \tag{1}$$

If we assume a spherical shape, we can distinguish "large" bodies, having radius $R \gg l_S$, for which thermal effects are limited to a thin surface shell, and "small" bodies with R smaller than or of the same order as l_S, for which temperature changes occur throughout the interior of the body. Note that ν can correspond either to a rotational frequency (ω, that is 2π over the rotational period, yielding a "diurnal" effect) or to the mean orbital motion n of the object around the source body (in our case the Sun, yielding a "seasonal" effect); in the former case, l_S is much smaller than in the latter. We will deal separately with the two types of effects in Section 3 below. Of course, in either case the solar radiation flux (and the corresponding temperature variations) will contain higher harmonics of the basic frequency ν, but these will cause only minor quantitative changes in our results.

Another thermal parameter is needed to specify how well the body retains significant temperature changes over a cycle of frequency ν. If $\tau = 2\pi/\nu$ and τ_{rel} is the temperature relaxation time over which infrared emission carries away the heat accumulated during a cycle τ, we can define "fast" radiation influx changes (corresponding to poor efficiency in building up temperature gradients across the body) as those with $\Theta = \tau_{rel}/\tau > 1$, and "slow" radiation influx changes (giving rise to large temperature gradients) as those with $\Theta < 1$. For the diurnal effect described above, this may be translated into a fast and a slow rotation regime, respectively (see, e.g., Spencer *et al.* 1989). To obtain a useful expression for Θ, we note that for large bodies (as defined above) the thermally affected surface shell contains a thermal energy $\approx 4\pi R^2 l_S \rho C T$ (T being the average temperature of the body), and radiates away an infrared energy flux $4\pi\varepsilon\sigma R^2 T^4$ (here ε is the surface infrared emissivity and σ the Stefan–Boltzmann constant), so that τ_{rel} is just the ratio between these two quantities. We end up with

$$\Theta = \frac{\sqrt{\rho C K}\sqrt{\nu}}{2\pi\varepsilon\sigma T^3}, \tag{2}$$

where $\sqrt{\rho C K}$ is the "thermal inertia" quantity used, e.g., by Spencer *et al.* 1989. The average temperature T can be estimated by the energy balance equation

$$\pi R^2(1 - A)S = 4\pi R^2 \varepsilon\sigma T^4, \tag{3}$$

where A is the surface albedo and S is the solar energy influx, that is, the solar constant $S_\oplus = 1370$ W m^{-2} times the squared semimajor axis ratio $(a_\oplus/a)^2$ between the Earth and the body under consideration. Thus we obtain

$$T^4 = \frac{(1 - A)S}{4\varepsilon\sigma}. \tag{4}$$

3. DIURNAL AND SEASONAL EFFECTS

As we have already anticipated, for a spinning body orbiting around the Sun there are two variants of the Yarkovsky effect, corresponding to the two typical time scales of the solar illumination cycle: the diurnal one due to the rotational motion and the seasonal one due to the orbital motion. The latter effect vanishes when the obliquity ζ (i.e., the angle between the polar axis and the perpendicular to the orbital plane) is zero, while the former one vanishes when $\zeta = 90°$. Simple diagrams showing the geometry of the perturbing force in both cases are given by Burns *et al.* (1979, p. 35) and Rubincam (1995, p. 1586, and 1998). Both effects become weaker when the corresponding Θ parameter grows to values $\gg 1$. Since we are mainly interested in semimajor axis changes due to the Yarkovsky force (the recoil force from anisotropically re-emitted thermal radiation), we need expressions for the along-track component of the force: if f_Y is the along-track component of the

Yarkovsky force per unit mass of the body, the corresponding semimajor axis drift for a near-circular orbit is simply $\dot{a} = 2f_Y/n$ (where n is the orbital mean motion, coinciding with the seasonal frequency discussed above).

For the diurnal effect we will use the expression for f_Y derived by Peterson (1976) for large bodies; in this case it is easy to show that this approximation is always valid (for rotation periods up to several hours) at sizes greater than about 10 cm, which are relevant for meteorites. On the other hand, for the seasonal effect the transition from small to large bodies occurs at a radius of about 10 m, so we need to deal with both cases. Therefore, we have rederived an expression of the seasonal perturbing force which is valid over the entire size range from ≈10 cm to 100 m.

Following Burns *et al.* (1979), in either case we can write

$$f_Y = \frac{2}{\rho R}\frac{\varepsilon\sigma T^4}{c}\frac{\Delta T}{T}f(\zeta), \tag{5}$$

where we are going to use different expressions for the effective temperature difference ΔT and for the obliquity function $f(\zeta)$ in the two cases. Rewriting Peterson's (1976) Eq. (26b) in our notation, for the "diurnal" Yarkovsky effect we have $f(\zeta) = \cos\zeta$ and

$$\frac{\Delta T_\omega}{T} = 0.667\frac{\Theta_\omega}{(1 + 2.03\,\Theta_\omega + 2.04\,\Theta_\omega^2)}, \tag{6}$$

where Θ_ω is the thermal parameter corresponding to the rotational frequency $\nu = \omega$ (apart from a numerical factor of order unity, this is the same as Peterson's P in his large body case). Peterson's result was derived by generalizing to a spherical geometry a thermal model developed in a cylindrical case; however, a self-consistent spherical model (Vokrouhlický 1998, in preparation) shows that Peterson's result is fairly accurate. Note that, as has been known for a long time (see, e.g., Öpik 1951), the diurnal Yarkovsky force produces a drag-like effect ($\dot{a} < 0$) for retrograde rotations ($\pi/2 < \zeta < \pi$), and *vice versa*. Also, as expected from our earlier discussion of the significance of the thermal parameter Θ, for large values of Θ_ω we have $\Delta T/T \propto \Theta_\omega^{-1}$ and the force drops to zero.

For the seasonal effect, according to Rubincam (1995) we have $f(\zeta) = -\sin^2\zeta$; that is, a drag-like effect is always produced, whose intensity depends on the obliquity. To compute the effective temperature difference to be substituted into Eq. (5), we have followed Rubincam (1987, 1998) and Afonso *et al.* (1995) in solving the heat conduction equation for a homogeneous spherical body with appropriate boundary conditions, by assuming that the surface temperature change δT is always $\ll T$ and that both the external irradiance and δT can be expressed as Fourier series of time. For the δT Fourier component corresponding to a frequency ν and to the degree-1 Legendre polynomial of latitude (which is the only one affecting the Yarkovsky force in this approximation), we have

$$\frac{\delta T}{T} = \frac{f_1(\nu)}{1+\tau}\frac{1}{1 + \dfrac{\tau}{1+\tau}\psi(kR)}, \tag{7}$$

to be compared with Eqs. (7) and (9) of Rubincam (1987), where we have substituted the expressions for the spherical Bessel function of degree 1 and its derivative. Here $\tau \equiv (\pi/2)(l_S/R)\Theta(\nu)$, $f_1(\nu)$ is the Fourier spectrum of the quantity $(S/2)\ \mathbf{r}\cdot\mathbf{s}$ (with $\mathbf{r}$ the heliocentric unit radius vector and $\mathbf{s}$ the rotation axis unit vector), and the function ψ of the complex variable z is given by

$$\psi(z) = \frac{(z^2 - 3)\sin z + 3z\cos z}{\sin z - z\cos z}, \tag{8}$$

with $z \equiv \sqrt{-i}(R/l_s)$. Then we have written the complex function appearing in the right-hand side of Eq. (7) as

$$\left[1 + \frac{\tau}{1+\tau}\psi(kR)\right]^{-1} = A_\nu\exp(i\delta_\nu), \tag{9}$$

and used the amplitude A_n and phase δ_n corresponding to the frequency $\nu = n$ to express the effective temperature change due to the seasonal effect as

$$\frac{\Delta T_n}{T} = \frac{1}{3}\frac{1}{1+\tau}A_n\sin\delta_n. \tag{10}$$

Finally this was inserted into Eq. (5), together with $f(\zeta) = -\sin^2\zeta$, to obtain f_Y. We have verified that our results match those obtained independently by Rubincam (1998) for the same case. We also note that an improved, nonlinearized thermal model (Vokrouhlický and Farinella, manuscript in preparation) gives results in fair agreement with those obtained above and those of Rubincam (1995, 1998) in the large body case, with a discrepancy of about 15% for the intensity of the force, and an exponent close to 1.9— instead of 2—in the $\sin^2\zeta$ factor.

4. SEMIMAJOR AXIS DRIFT RATES

In order to estimate the rate of the Yarkovsky-driven semimajor axis drift as a function of size, we still need estimates both for the relevant thermal/physical properties for meteoritic/asteroidal material (ρ, C, K, A, ε) and for the rotation rates and their size dependence. As for the former quantities, we have assumed $A = 0$, $\varepsilon = 1$ for the sake of simplicity, whereas three sets of representative values of K, C, and ρ for stony, metal-rich, and regolith-

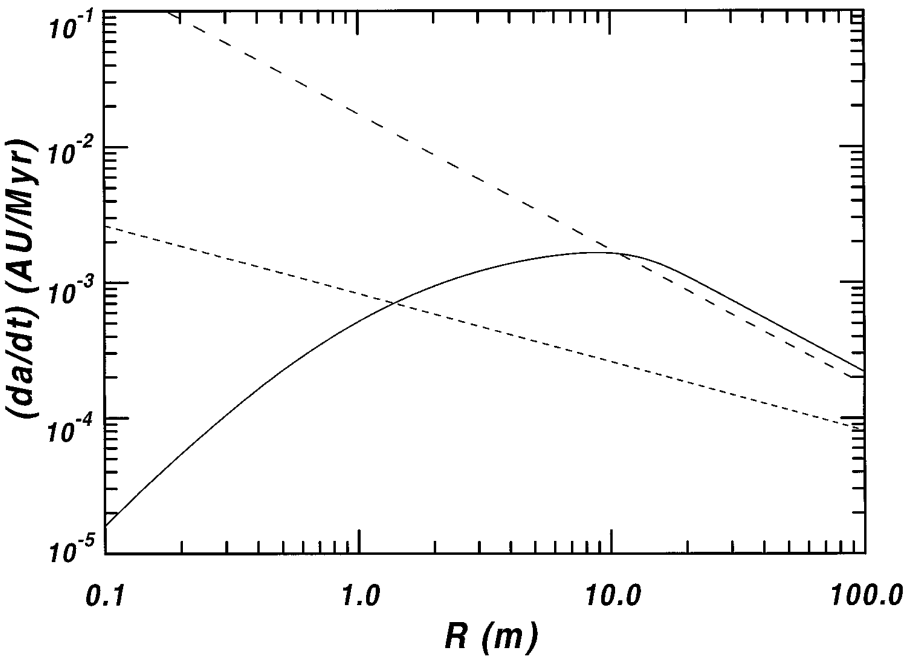

FIG. 1. The maximum semimajor axis drifts vs size for bare basalt fragments at $a = 2$ AU. The full line corresponds to the seasonal effect for $\zeta = 90°$, the long-dashed line to the diurnal effect assuming a size-independent spin period of 5 h, and the short-dashed line to the diurnal effect with $\omega \propto R^{-1}$. Diurnal effects are calculated for $\zeta = 0$.

covered bodies are listed in Table I; these values are the same adopted by Rubincam (1995) for basaltic and regolith-covered bodies, and by Burns *et al.* (1979) for metal-rich objects.

As for the spin rates, we shall make two different assumptions: (i) a size-independent spin period of 5 h, close to the average value for small asteroids (see, e.g., Binzel *et al.* 1989, Harris 1996), as previously assumed by Peterson (1976); and (ii) a spin period of 5 hr $\times$ ($2R$/1 km). In our opinion, assumption (ii) is more realistic, because at 0.1–1 km diameter the transition between gravitationally bound "piles of rubble" and competent fragments is likely to occur among asteroids (Love and Ahrens 1996, Melosh and Ryan 1997), and for solid fragments a linear relationship between period and size is supported by both laboratory data from breakup experiments (Fujiwara and Tsukamoto 1981, Fujiwara 1987, Yaganisawa *et al.* 1991, Giblin *et al.* 1994) and theoretical modeling (Harris 1979, Paolicchi *et al.* 1989). The above relationship yields spin periods of a few seconds for cm-sized bodies, in agreement with experimental results. We also note that according to Adolfsson (quoted in Ceplecha 1996), the spin period of the meter-sized Lost City bolide has been determined to be 3.3 $\pm$ 0.3 s, which is comparable to that inferred from our suggested relationship.

Figure 1 shows the Yarkovsky-driven $\dot{a}$ (in AU/Myr) as a function of R, at $a = 2$ AU and using basalt-like material properties. The three curves correspond to the seasonal effect (the solid one bending down on the left side) and to the diurnal effect with size-independent ω and with $\omega \propto 1/R$ (long- and short-dashed lines, respectively). In the seasonal case, at sizes smaller than $\approx$10 m f_Y and $\dot{a}$ start decreasing owing to the onset of the small body regime, in which the decrease of ΔT more than compensates for the larger area-to-mass ratio. In all cases we have taken $f(\zeta) = 1$, corresponding to the maximum amplitude of f_Y: if collisions reorient the spin axis frequently enough, the seasonal effect will yield a secular semimajor axis decay at an average rate $\approx$2/3 of that shown in Fig. 1 (assuming that all spin axis positions are equally likely), whereas the diurnal effect will just cause a random walk in a.

Taking this into account (see Section 5), plus the fact that the $\omega \propto 1/R$ relationship (short-dashed line) looks more plausible, we conclude that at sizes of interest for meteorites and their immediate parent bodies ($\approx$1 to 10 m) the seasonal effect is likely to yield the dominant long-term orbit decay, corresponding to $\dot{a} \approx 10^{-3}$ AU/Myr. On this average trend, a random-walk behavior is probably superimposed, owing to the diurnal effect. The latter is probably dominant at $R \approx 0.1$ m.

Of course, the rates shown in Fig. 1 depend also on semimajor axis and composition. As for the dependence on a, it is not a very sensitive one: as shown in Fig. 2, the changes in the seasonal $\dot{a}$ values when one moves from 3 to 1 AU are very small in the large body regime and reach about a factor of 10 at sizes of about 1 m. For metal-rich

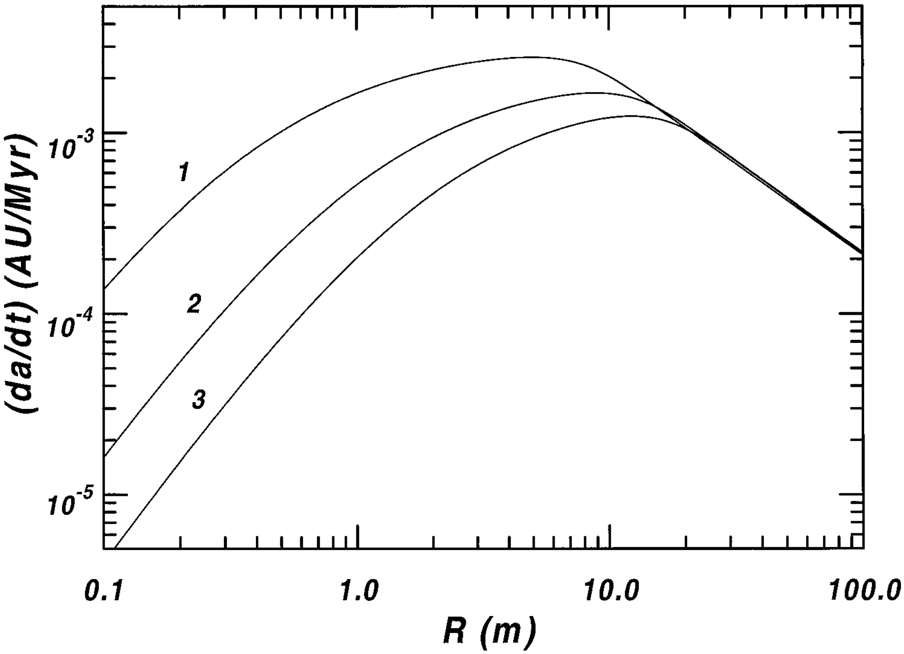

FIG. 2. The seasonal semimajor axis drift shown in Fig. 1 at $a = 2$ AU has been replotted here for the range of semimajor axes between 1 and 3 AU. The labels of the curves correspond to semimajor axes in AU.

bodies, the drift rates are in general lower than for stones: the difference is only about a factor of 2 in the large body (R larger than about 30 m) seasonal case, but it becomes much larger for small bodies and is about one order of magnitude for the diurnal effect (see Fig. 3). In the metal-rich case, the diurnal effect is already the dominant one at $R \approx 1$ m.

The situation is quite different when one considers regolith-covered bodies. As remarked by Rubincam (1995), assuming the lunar-like regolith parameters given in Table I, a relatively thin regolith is enough to affect the thermal conductivity in the critical surface layer of the bodies. For the seasonal effect, Eq. (1) yields a critical thickness of $\approx$10 cm. We believe that such regoliths are unlikely on meter-sized bodies (relevant for meteorites), because of their negligible self-gravity and likely rapid rotation (resulting into loss of ejecta or loose surface material), but may exist on objects $\approx$100 m in diameter and larger, for which gravitational effects are important in determining their response to collisions (Love and Ahrens 1996).

However, for the diurnal effect the critical regolith thickness is only $\approx$1 mm for spin periods of order 1 h, and even less for faster rotations, owing to the $\nu^{-1/2}$ factor in Eq. (1). It seems possible (although by no means certain) that even meter-sized meteoroids could develop such a thin surface layer of dusty or porous material with a relatively low thermal conductivity. As shown in Fig. 4 (corresponding again to $a = 2$ AU and $f(\zeta) = 1$), for regolith-covered bodies the diurnal effect is the dominant one at all sizes. At diameters $\approx$100 m typical $\dot{a}$ values are $\approx 10^{-3}$ AU/Myr. Meter–sized regolith–covered stones would drift faster, at typical rates of a few hundredths AU/Myr. Note that Fig. 4 was plotted by assuming the regolith parameters of Table I, but a basalt-like bulk density; for irons, with the same regolith properties, $\dot{a}$ values would be about a factor of two smaller due to the higher bulk density.

5. COLLISIONAL TIME SCALES

The Yarkovsky orbital drift is limited by the fact that small asteroids have collisional lifetimes much shorter than the age of the solar system (Davis *et al.* 1989). Moreover, as we have already noted, the orbital effects of the two variants of the Yarkovsky force have some important differences: (1) the seasonal mechanism always yields drag-like effects (i.e., a secular decay) for the semimajor axis, whose intensity depends on the obliquity of the spin axis, whereas the orbital eccentricity can be either increased or decreased (Vokrouhlický and Farinella 1998, in preparation); (2) the semimajor axis effect of the diurnal mechanism changes in sign when the rotation axis is reversed and the spin is changed from prograde to retrograde, or *vice versa*, by a collision. Therefore, collisions interact in an important way with the Yarkovsky orbital effects and are especially important for regolith-covered bodies (domi-

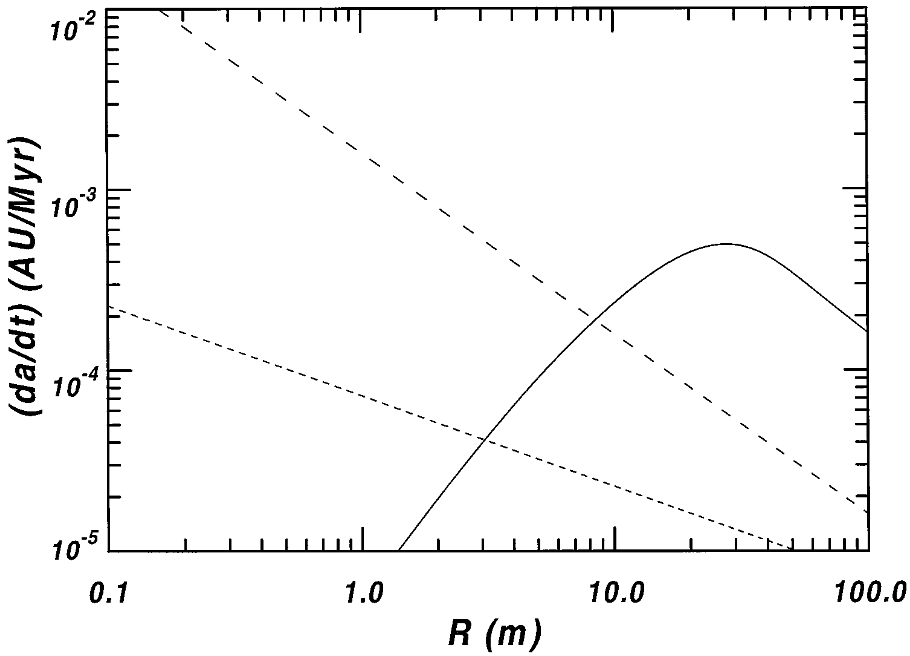

FIG. 3. The same as Fig. 1 but for bare iron-rich fragments (parameters given in Table 1).

nated by the diurnal effect). Here, we shall try to estimate the relevant collisional time scales.

As for impact disruption, the typical collisional lifetime for a target of radius R can be expressed as

$$\tau_{\rm disr} = \frac{1}{P_i R^2 N(r_{\rm disr})}, \tag{11}$$

where P_i is the intrinsic collision probability according to Wetherill (1967) and $N(r_{\rm disr})$ is the number of asteroids of radius exceeding the minimum value $r_{\rm disr}$ which is required to shatter the target. The average value of P_i in the asteroid belt is 2.85×10^{-18} km^{-2} yr^{-1} (Farinella and Davis 1992). According to Davis *et al.* (1989), $r_{\rm disr}$ is related to the impact strength S of the target, the material density ρ_p of the projectile, and the average collision velocity V by

TABLE I
Thermal Parameters for Different Materials

	ρ (kg/m^3)	K (W/m/K)	C (J/kg/K)
Basalt	3500	2.65	680
Iron-rich	8000	40	500
Regolith-covered	1500	0.0015	680

Note. The entries have been taken from Rubincam (1995) for basaltic and regolith-covered bodies and from Burns *et al.* (1979) for metal-rich objects.

$$r_{\rm disr} = \left(\frac{4S}{\rho_p V^2}\right)^{1/3} R. \tag{12}$$

Here we can take as reasonable values $V = 5.8$ km/s (Farinella and Davis 1992, Bottke *et al.* 1994a), $\rho_p = 2500$ kg/m^3 (Belton *et al.* 1995), and $S = 3 \times 10^6$ J/m^3 (for silicate targets; see Fijiwara *et al.* 1989) or 5×10^8 J/m^3 (for metals; Davis and Ryan 1997, private communication). Finally, for the size distribution of small asteroids we assume that the number of bodies of radius $>r$ is

$$N(r) = 3.5 \times 10^5 \left(\frac{r}{1\ {\rm km}}\right)^{-5/2} \tag{13}$$

(see Farinella and Davis 1994 for a discussion of the normalizing factor; the $-5/2$ exponent is consistent with collisional steady state according to Dohnanyi 1969). The resulting collisional lifetimes are

$$\tau_{\rm disr} = 2.0 \times 10^7\ {\rm yr} \left(\frac{R}{1\ {\rm m}}\right)^{1/2} \tag{14}$$

for silicate bodies and

$$\tau_{\rm disr} = 1.4 \times 10^9\ {\rm yr} \left(\frac{R}{1\ {\rm m}}\right)^{1/2} \tag{15}$$

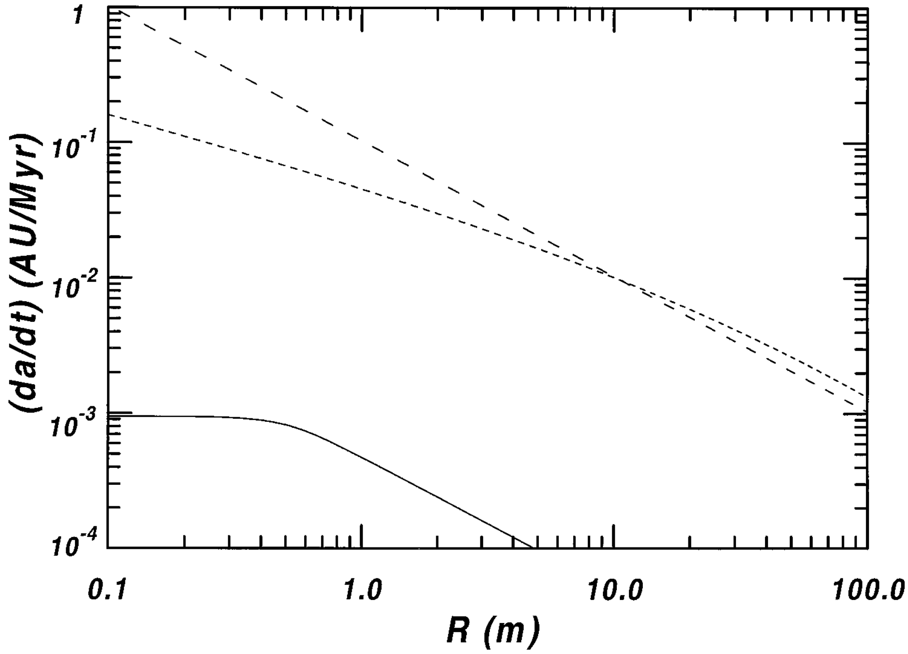

FIG. 4. The same as for Fig. 1 but for regolith-covered bodies. Here we have used the regolith thermal parameters given in Table I, but a bulk density of 3500 kg/m^3.

for irons. Although several parameters used for these estimates are quite uncertain, the fact that the resulting values of $\tau_{\rm disr}$ are comparable to the cosmic ray exposure (CRE) ages of stony and iron meteorites (see Section 6) raises the possibility that collisions do in fact control the CRE ages and suggests that the above calculation gives the correct order of magnitude for the collision time scales. Note also that Eq. (12) yields a lifetime $\approx 10^9$ yr for a 10-km asteroid such as 951 Gaspra, in good agreement with estimates by the Galileo team (Belton *et al.* 1992) and other workers (Farinella *et al.* 1992, Greenberg *et al.* 1994).

Now, in order to completely change the spin axis of a body, the angular momentum of the projectile must be comparable to the preimpact rotational angular momentum of the target. If the target's spin rate and density are ω and ρ_t, the radius of the required projectile is

$$r_{\rm rot} = \left(\frac{2\sqrt{2}\rho_t\omega R}{5\rho_p V}\right)^{1/3} R. \quad (16)$$

The corresponding time scale $\tau_{\rm rot}$, computed as above but using $N(r_{\rm rot})$ instead of $N(r_{\rm disr})$ in Eq. (9), is

$$\tau_{\rm rot} = 1.88 \times 10^4 \text{ yr} \left(\frac{R}{1 \text{ m}}\right)^{4/3} \quad (17)$$

if we assume a size–independent rotational period of 5 h and

$$\tau_{\rm rot} = 3.34 \times 10^6 \text{ yr} \left(\frac{R}{1 \text{ m}}\right)^{1/2} \quad (18)$$

if we assume $\omega \propto R^{-1}$ and a period of 5 h at a diameter of 1 km. These estimates have been obtained by assuming $\rho_t = \rho_p$; for iron bodies a better assumption is $\rho_t/\rho_p \approx 3$, and the lifetimes (15) and (16) should be increased by a factor $3^{5/6} \approx 2.5$. Also, we have neglected any angular momentum carried away by impact ejecta; if angular momentum loss is important, $\tau_{\rm rot}$ might be somewhat longer than estimated above.

These results indicate that spin axis reorientation is very frequent (compared to the collisional lifetime) in the constant-ω case, but is also likely to occur several times in a collisional lifetime in the more realistic $\omega \propto R^{-1}$ case. This implies that: (i) when the seasonal effect is the dominant one (that is, for bare fragments larger than $\approx$1 m; see Fig. 1), taking the average value 2/3 for the $\sin^2 \zeta$ factor gives the correct average value of $\dot{a}$; (ii) when the diurnal effect is the dominant one (e.g., for regolith-covered surfaces), the semimajor axis evolution is likely to resemble a real random walk and the body is expected to move (in either direction) by an amount roughly proportional to the square root of the elapsed time.

For instance, according to Eqs. (14) and (18), for a 1-m radius stony fragment about six spin-reorienting events are expected within the collisional lifetime $\tau_{\rm disr}$, and therefore the fragment is typically shifted by two or three times the distance covered over a timestep $\tau_{\rm rot}$. Figures 1 and 4 show that this typical shift is <0.01 AU for bare fragments, but ≈0.1 AU if they have a thin regolith. The corresponding typical shift for irons is larger, because the longer collisional lifetime more than compensates for the slower random-walk evolution. Also, 100-m stony bodies may survive for ≈100 Myr vs collisional disruption without frequent spin axis changes, which suggests that even at a rate of $\approx 10^{-3}$ AU/Myr the diurnal Yarkovsky effect may play a significant role in their delivery to Earth-crossing orbits, provided some regolith is present on their surfaces.

As is clear from this discussion, orbital evolution under Yarkovsky effects is a complex process, due to the different size dependence of the diurnal and seasonal variants and the sensitivity to thermal properties and the possible presence of a regolith. Moreover, the Yarkovsky drift has an intrinsically stochastic character associated with collisional events: since collisions affect the rotation rates and spin axes, they can change the pace of the orbital evolution and even, in some cases, the relative importance of the seasonal and diurnal modes.

6. IMPLICATIONS FOR METEORITES

Both the observed CRE ages (Caffee *et al.* 1988, Marti and Graf 1992) and the estimated collision rates (Eqs. (14) and (15) above) suggest that in the main belt the lifetimes of small stony asteroids vs collisional disruption range from ≈10 to 50 Myr for sizes between 1 and 10 m; similar iron bodies typically survive for times of several hundred Myr to a few Byr. Together with the semimajor axis drift rates discussed in Sections 4 and 5, this implies that the Yarkovsky effects may provide these bodies with significant semimajor axis mobility. For regolith-free fragments (Figs. 1 and 3), the combination of seasonal decay and diurnal random walk can probably shift semimajor axes by a few hundredths AU between two breakup events. If a thin, poorly conductive regolith layer is present (Fig. 4), the diurnal effect may move the orbits farther, by ≈0.1 AU. It is likely that iron bodies are more mobile (if slower) than stones, due to their much longer collisional lifetimes.

Now, in the main asteroid belt the most prominent gaps associated with secular and mean motion resonances are located at $a \approx 2.1$, 2.5, 2.8, and 3.3 AU, and therefore the typical distance to a nearby Kirkwood gap (or secular resonance) is ≈0.2 AU. This suggests that the Yarkovsky effect is probably important in delivering asteroid fragments to resonances and removing them from the main belt population. This possibility was mentioned in passing by Rubincam (1995, p. 1592), but was not elaborated upon in that paper.

Actually, more modeling work needs to be done to clarify the interaction between the Yarkovsky effect and collisions for small main-belt objects. Collisions erode and shatter the bodies, thus reducing their size and also reorient the spin axis, affecting the Yarkovsky drift rate. However, the existence and nature of the impact-induced effects (both disruption and reorientation) is a complex, nonlinear problem. The rate of impacts depends on the number density of smaller objects, and if the smaller objects are efficiently cleared from the belt, the rate would be lower and objects would move more efficiently toward the resonances, hence maintaining the low impact rate—a feedback effect.

Meteorite CRE data and size distributions suggest that most preatmosphere meteorite bodies are in the 1-m size range—near the size that is most affected by Yarkovsky forces. The conventional non-Yarkovsky delivery mechanism of this material from main-belt parent asteroids to resonances (where the orbital eccentricity is rapidly pumped up to Earth-crossing values by planetary perturbations) is directly by collision-induced ΔV, resulting into instantaneous orbital element changes (see Farinella *et al.* 1993a and references therein). But there are now some convincing arguments to support the alternative view that many meteorites stay in the main belt for comparatively long times, undergoing a slow Yarkovsky-driven semimajor axis drift, after being collisionally ejected from their parent bodies and before ending up in a resonance.

As a consequence, the Yarkovsky effect could solve a conundrum concerning meteorite ages. Recent dynamical work (e.g., Farinella *et al.* 1993b, 1994, Valsecchi *et al.* 1995, Migliorini *et al.* 1997a, Gladman *et al.* 1997) has shown that, once in the chaotic zone associated to a resonance (either the ν_6, secular, or the 3 : 1, jovian mean motion, at $a \approx 2.1$ and 2.5 AU, respectively), asteroid fragments have a dynamical lifetime of only a few Myr before falling into the Sun or being ejected from the solar system by a Jupiter encounter. Only along the edges of the main gaps or within higher-order resonances can some "sticky" regions be found with longer orbital evolution time scales (see, e.g., Milani and Farinella 1995), but the volume in orbital element space of the chaotic regions where typical lifetimes are in the range from 10^7 to 10^9 yr appears to be very small. Moreover, even when asteroid fragments are extracted from the resonances by planetary close encounters and attain semimajor axes in the inner planet region (<2 AU), their dynamical lifetimes are of the order of 10^7 yr only (Gladman *et al.* 1995, 1996, 1997).

These dynamical lifetimes are shorter than the CRE ages of most meteorites. Typical CRE ages are a few tens of Myr for ordinary chondrites and HEDs and 10^8–10^9 yr for irons; in both cases CRE ages shorter than a few Myr are very rare. Note that CRE ages give just a lower bound on the time since a meteoroid has been ejected from its asteroidal parent, since they only measure the time scale over which the material has stayed buried at a depth of the order of a meter or less (Caffee *et al.* 1988). For instance, for L-chondrites Ar–Ar impact ages and other data strongly suggest a common origin from the disruption of a sizeable parent asteroid some 500 Myr ago (Haack *et al.* 1996)—

after which, several generations of smaller collisions have resulted in the current meteorites (probably giving rise to complex exposure histories; see Wetherill 1980). But such later disruptive collisions are not very efficient in moving debris toward resonances, because typical fragment ejection velocities do not exceed 10–100 m/s (corresponding to semimajor axis shifts of only 0.001–0.01 AU) and have random directions. Therefore we believe that the comparatively old ages of meteorites (in particular irons) can be reconciled with the short dynamical lifetimes in the resonances only by assuming that the corresponding asteroid fragments have been drifting slowly and for comparatively long times in main-belt nonresonant orbits, before eventually "falling" into short-lived resonant escape hatches. In such a scenario, the near-absence of meteorites with very short CRE ages may be due to the stochastic and discrete nature of asteroidal collisional events.

Also, when coupled to Yarkovsky-driven mobility the much longer collisional lifetimes of iron fragments may explain why ordinary chondrites appear to come from a small number of sizeable parent asteroids, probably located near the edges (say, within several hundredths of AU) of the resonances, such as 6 Hebe (Farinella *et al.* 1993a,b, Morbidelli *et al.* 1994, Gaffey 1996, Migliorini *et al.* 1997b), whereas iron meteorites sample a larger number (up to several tens) of presumably smaller parent asteroids (Scott and Wasson 1975, Wasson 1990, Keil *et al.* 1994). Also, Hartmann *et al.* (1997) have noted that due to the longer lifetimes and the slower Yarkovsky drift of irons compared to stones, the relative abundance of small iron fragments in the main asteroid belt is probably higher than that of stones. In other words, the belt would be depleted in meter-scale stones, which are more rapidly ejected toward planets, and the Earth could receive an excess of stones by this mechanism, compared to irons (although the recovery rate of iron meteorites on the Earth's surface is higher because of lesser atmospheric ablation, higher resistance to weathering, and greater ease of identification).

Finally, as remarked by Rubincam (1995, 1998), the Yarkovsky effect may play a significant role in delivering to Earth-crossing orbits asteroid fragments 10 to 100 m in size, especially if their surfaces are covered by regolith layers. The orbital distribution of these Tunguska-like bodies in the near-Earth region is still poorly known and understood (see, e.g., Rabinowitz 1993, 1994, Bottke *et al.* 1996, Farinella and Menichella 1998), and it is possible that the Yarkovsky effect will prove to be an important ingredient of their dynamics. According to the estimates of Sections 4 and 5, regolith-covered 100-m sized bodies may move by $\approx$0.1 AU in a random direction before being disrupted, and therefore the Yarkovsky effect might be responsible for injecting many of them into the resonances. The Yarkovsky orbital drift may become even more important when the aphelia of these bodies become decoupled from the main asteroid belt (i.e., become $<$1.7 AU), since in this case the collisional time scales are much longer (Bottke *et al.* 1994b). However, we believe that further work is needed to model the orbital evolution of these objects, for which a dominant diurnal effect results in a semimajor axis random walk and a complex interplay is present between gravitational and nongravitational effects.

ACKNOWLEDGMENTS

We acknowledge helpful reviews by G. W. Wetherill and D. P. Rubincam. The latter reviewer in particular suggested to us how to deal correctly with the "small body" case and provided us with an unpublished plot with which we could compare our results. We are also grateful to the late F. Migliorini, Z. Ceplecha, D. R. Davis, Ch. Froeschlé, B. Gladman, F. Marzari, A. Morbidelli, E. Ryan, and S. J. Weidenschilling for helpful discussions and comments. P. F. acknowledges support from the Italian Space Agency (ASI) and the Italian Ministry for University and Scientific Research (MURST). This is PSI Contribution 342.

REFERENCES

Afonso, G., R. S. Gomes, and M. A. Florczak 1995. Asteroid fragments in Earth-crossing orbits. *Planet. Space Sci.* **43,** 787–795.

Belton, M. J. S., J. Veverka, P. Thomas, P. Helfenstein, D. Simonelli, C. Chapman, M. E. Davies, R. Greeley, R. Greenberg, J. Head, S. Murchie, K. Klaasen, T. V. Johnson, A. McEwen, D. Morrison, G. Neukum, F. Fanale, C. Anger, M. Carr, and C. Pilcher 1992. Galileo encounter with 951 Gaspra: First pictures of an asteroid. *Science* **257,** 1647–1652.

Belton, M. J. S., C. R. Chapman, P. C. Thomas, M. E. Davies, R. Greenberg, K. Klaasen, D. Byrnes, L. D'Amario, S. Synnott, T. V. Johnson, A. McEwen, W. J. Merline, D. R. Davis, J.-M. Petit, A. Storrs, J. Veverka, and B. Zellner 1995. Bulk density of asteroid 243 Ida from the orbit of its satellite Dactyl. *Nature* **374,** 785–788.

Binzel, R. P., P. Farinella, V. Zappalà, and A. Cellino 1989. Asteroid rotation rates: Distributions and statistics. In *Asteroids II* (R. P. Binzel, T. Gehrels, and M. S. Matthews, Eds.), pp. 416–441, Univ. of Arizona Press, Tucson.

Bottke, W. F., M. C. Nolan, R. Greenberg, and R. A. Kolvoord 1994a. Velocity distributions among colliding asteroids. *Icarus* **107,** 255–268.

Bottke, W. F., M. C. Nolan, R. Greenberg, and R. A. Kolvoord 1994b. Collisional lifetimes and impact statistics of near-Earth asteroids. In *Hazards Due to Comets and Asteroids* (T. Gehrels, Ed.), pp. 337–357, Univ. of Arizona Press, Tucson.

Bottke, W. F., M. C. Nolan, H. J. Melosh, A. M. Vickery, and R. Greenberg 1996. Origin of the Spacewatch small Earth-approaching asteroids. *Icarus* **122,** 406–427.

Burns, J. A., P. L. Lamy, and S. Soter 1979. Radiation forces on small particles in the Solar System. *Icarus* **40,** 1–48.

Caffee, M. W., J. N. Goswami, C. M. Hohenberg, K. Marti, and R. C. Reedy 1988. Irradiation records in meteorites. In *Meteorites and the Early Solar System* (J. F. Kerridge and M. S. Matthews, Eds.), pp. 205–245, Univ. of Arizona Press, Tucson.

Ceplecha, Z. 1996. Luminous efficiency based on photographic observations of the Lost City fireball and implications for the influx of interplanetary bodies onto Earth. *Astron. Astrophys.* **311,** 329–332.

Davis, D. R., S. J. Weidenschilling, P. Farinella, P. Paolicchi, and R. P. Binzel 1989. Asteroid collisional history: Effects on sizes and spins. In *Asteroids II* (R. P. Binzel, T. Gehrels, and M. S. Matthews, Eds.), pp. 805–826, Univ. of Arizona Press, Tucson.

Dohnanyi, J. S. 1969. Collisional model of asteroids and their debris. *J. Geophys. Res.* **74,** 2531–2554.

Farinella, P., and D. R. Davis 1992. Collision rates and impact velocities in the main asteroid belt. *Icarus* **97,** 111–123.

Farinella, P., and D. R. Davis 1994. Will the real asteroid size distribution please step forward. *Lunar Planet. Sci. Conf.* **XXV,** 365–366.

Farinella, P., and D. Vokrouhlický 1996. Thermal force effects on slowly rotating, spherical artificial satellites. I. Solar heating. *Planet. Space Sci.* **44,** 1551–1561.

Farinella, P., and M. Menichella 1998. The flux of Tunguska-sized fragments from the main asteroid belt. *Planet. Space Sci.*, in press. [Proc. Tunguska 96 Conference, Bologna, July 1996]

Farinella, P., D. R. Davis, A. Cellino, and V. Zappalà 1992. The collisional lifetime of asteroid 951 Gaspra. *Astron. Astrophys.* **257**, 329–330.

Farinella, P., R. Gonczi, Ch. Froeschlé, and C. Froeschlé 1993a. The injection of asteroid fragments into resonances. *Icarus* **101,** 174–187.

Farinella, P., Ch. Froeschlé, and R. Gonczi 1993b. Meteorites from the asteroid 6 Hebe. *Celest. Mech.* **56,** 287–305.

Farinella, P., Ch. Froeschlé, C. Froeschlé, R. Gonczi, G. Hahn, A. Morbidelli, and G. B. Valsecchi 1994. Asteroids falling into the Sun. *Nature* **371,** 314–317.

Farinella, P., D. Vokrouhlický, and F. Barlier 1996. The rotation of LAGEOS and its long-term semimajor axis decay: A self-consistent solution. *J. Geophys. Res.* **101**(B8), 17,861–17,872.

Fujiwara, A. 1987. Energy partition into translational and rotational motion of fragments in catastrophic disruption by impact: An experiment and asteroid cases. *Icarus* **70,** 536–545.

Fujiwara, A., and A. Tsukamoto 1981. Rotation of fragments in catastrophic impact. *Icarus* **48,** 329–334.

Fujiwara, A., P. Cerroni, D. R. Davis, E. Ryan, M. Di Martino, K. Holsapple, and K. Housen 1989. Experiments and scaling laws on catastrophic collisions. In *Asteroids II* (R. P. Binzel, T. Gehrels, and M. S. Matthews, Eds.), pp. 240–265, Univ. of Arizona Press, Tucson.

Gaffey, M. J. 1996. Asteroid 6 Hebe: Spectral evaluation of the prime large mainbelt ordinary chondrite parent body candidate, with implications from space weathering of Gaspra and the Ida–Dactyl system. *Lunar Planet Sci.* **XXVII,** 391–392.

Giblin, I., G. Martelli, P. N. Smith, A. Cellino, M. Di Martino, V. Zappalà, P. Farinella, and P. Paolicchi 1994. Field fragmentation of macroscopic targets simulating asteroidal catastrophic collisions. *Icarus* **110,** 203–224.

Gladman, B. J., J. A. Burns, M. Duncan, and H. F. Levison 1995. The dynamical evolution of lunar impact ejecta. *Icarus* **118,** 302–321.

Gladman, B. J., J. A. Burns, M. Duncan, P. Lee, and H. F. Levison 1996. The exchange of impact ejecta between terrestrial planets. *Science* **271,** 1387–1392.

Gladman, B. J., F. Migliorini, A. Morbidelli, V. Zappalà, P. Michel, A. Cellino, Ch. Froeschlé, H. F. Levison, M. Bailey, and M. Duncan 1997. Dynamical lifetimes of objects injected into asteroid belt resonances. *Science* **277,** 197–201.

Greenberg, R., and M. C. Nolan 1989. Delivery of asteroids and meteorites to the inner Solar System. In *Asteroids II* (R. P. Binzel, T. Gehrels, and M. S. Matthews, Eds.), pp. 778–804, Univ. of Arizona Press, Tucson.

Greenberg, R., M. C. Nolan, W. F. Bottke, R. A. Kolvoord, and J. Veverka 1994. Collisional history of Gaspra. *Icarus* **107,** 84–97.

Haack, H., P. Farinella, E. R. D. Scott, and K. Keil 1996. Meteoritic, asteroidal, and theoretical constraints on the 500 Ma disruption of the L chondrite parent body. *Icarus* **119,** 182–191.

Harris, A. W. 1979. Asteroid rotation rates. II. A theory for the collisional evolution of rotation rates. *Icarus* **40,** 145–153.

Harris, A. W. 1996. The rotation rates of very small asteroids: Evidence for ''rubble pile'' structure. *Lunar Planet. Sci. Conf.* **XXVII,** 493–494.

Hartmann, W. K., P. Farinella, S. Weidenschilling, E. Ryan, D. Vokrouhlický, F. Marzari, D. Spaute, and D. R. Davis 1997. Yarkovsky effects: Possible consequences on meteorites and asteroids. *Lunar Planet. Sci. Conf.* **XXVIII,** 517–518.

Keil, K., H. Haack, and E. R. D. Scott 1994. Catastrophic fragmentation of asteroids: Evidence from meteorites. *Planet. Space Sci.* **42,** 1109–1122.

Love, S. G., and T. J. Ahrens 1996. Catastrophic impacts on gravity dominated asteroids. *Icarus* **124,** 141–155.

Marti, K., and T. Graf 1992. Cosmic–ray exposure history of ordinary chondrites. *Ann. Rev. Earth Planet. Sci.* **20,** 221–243.

Melosh, H. J., and E. V. Ryan 1997. Asteroids: Shattered but not dispersed. *Icarus* **129,** 562–564.

Migliorini. F., A. Manara, F. Scaltriti, P. Farinella, A. Cellino, and M. Di Martino 1997b. Surface properties of 6 Hebe: A possible parent body of ordinary chondrites. *Icarus* **128**, 104–113.

Migliorini, F., A. Morbidelli, V. Zappalà, B. J. Gladman, M. E. Bailey, and A. Cellino 1997a. Vesta fragments from ν_6 and 3:1 resonances: Implications for V–type NEAs and HED meteorites. *Meteoritics*, submitted. [Proc. Vesta/HED workshop, Houston, October 1996]

Milani, A., and P. Farinella 1995. An asteroid on the brink. *Icarus* **115,** 209-212.

Morbidelli, A., R. Gonczi, Ch. Froeschlé, and P. Farinella 1994. Delivery of meteorites through the ν_6 secular resonance. *Astron. Astrophys.* **282,** 955–979.

Öpik, E. J. 1951. Collision probabilities with the planets and the distribution of interplanetary matter. *Proc. Roy. Irish Acad.* **54,** 165–199.

Paolicchi, P., A. Cellino, P. Farinella, and V. Zappalà 1989. A semiempirical model of catastrophic breakup processes. *Icarus* **77,** 187–212.

Peterson, C. 1976. A source mechanism for meteorites controlled by the Yarkovsky effect. *Icarus* **29,** 91–111.

Rabinowitz, D. L. 1993. The size distribution of the Earth-approaching asteroids. *Astrophys. J.* **407,** 412–427.

Rabinowitz, D. L. 1994. The size and shape of the near-Earth asteroid belt. *Icarus* **111,** 364–377.

Radzievskii, V. V. 1952. A mechanism for the disintegration of asteroids and meteorites. *Astron. Zh.* **29,** 162–170. [in Russian]

Rubincam, D. P. 1987. LAGEOS orbit decay due to infrared radiation from Earth. *J. Geophys. Res.* **92,** 1287–1294.

Rubincam, D. P. 1988. Yarkovsky thermal drag on LAGEOS. *J. Geophys. Res.* **93,** 13,805–13,810.

Rubincam, D. P. 1995. Asteroid orbit evolution due to thermal drag. *J. Geophys. Res.* **100,** 1585–1594.

Rubincam, D. P. 1998. Yarkovsky thermal drag on small asteroids and Mars–Earth delivery. *J. Geophys. Res.—Planets* **103,** 1725–1732.

Scott, E. R. D., and J. T. Wasson 1975. Classification and properties of iron meteorites. *Rev. Geophys. Space Phys.* **13,** 527–546.

Spencer, J. R., L. A. Lebofsky, and M. V. Sykes 1989. Systematic biases in radiometric diameter determinations. *Icarus* **78,** 337–354.

Valsecchi, G. B., A. Morbidelli, R. Gonczi, P. Farinella, Ch. Foeschlé, and C. Froeschlé 1995. The dynamics of objects in orbits resembling that of P/Encke. *Icarus* **118,** 169–180.

Vokrouhlický, D., and P. Farinella 1997. Thermal force effects on slowly rotating, spherical artificial satellites. II. Earth infrared heating. *Planet. Space Sci.* **45,** 419–425.

Wasson, J. T. 1990. Ungrouped iron meteorites in Antarctica: Origin of anomalously high abundance. *Science* **249,** 900–902.

Wetherill, G. W. 1967. Collisions in the asteroid belt. *J. Geophys. Res.* **72,** 2429–2444.

Wetherill, G. W. 1980. Multiple cosmic-ray exposure ages of meteorites. *Meteoritics* **15,** 386–387.

Yaganisawa, M., J. Eluszkiewicz, and T. J. Ahrens 1991. Angular momentum transfer in low velocity oblique impacts: Implications for asteroids. *Icarus* **94,** 272–282.